

Synthesis, Characterization and Antimicrobial Activity (Biofilms) of *Boswellia Ovalifoliolata* Bark Extract Mediated AgNps and its Anticancer Efficacy

Supraja N.,*^a Rajasekhar K.K.,^b Kishore B.^c and Bhavitha J.^b

^aAcharya N G Ranga Agricultural University, Institute of Frontier Technology, R.A.R.S, Nanotechnology laboratory, Tirupathi-517507, India.

^bDepartment of Pharmaceutical Analysis, Sri Padmavathi School of Pharmacy, Tiruchanoor, Tirupati-517503, India.

^cDepartment of Pharmaceutics, Sri Padmavathi School of Pharmacy, Tiruchanoor, Tirupati-517503, India.

*Corresponding author E-mail address: krishna.supraja@gmail.com (Supraja N)

ISSN: 2582-3353



Publication details

Received: 01st September 2021

Revised: 19th October 2021

Accepted: 19th October 2021

Published: 2nd November 2021

Abstract: The biological synthesis of AgNPs is cost effective and eco-friendly to that of conventional method of nanoparticles synthesis. In this study, microbiological aspects of scale formation in PVC pipelines bacteria and fungi were isolated to evaluate antibacterial and antifungal activities through biosynthesis of AgNPs using bark extract of *Boswellia ovalifoliolata*. Stable AgNPs were formed by treatment of aqueous solution of AgNO₃ (1mM). The formation of BAgNPs was confirmed by UV– analysis and recorded the localized surface plasmon resonance (LSPR) at 430nm. FT-IR analysis revealed that primary and secondary amine groups in combination with the proteins present in the bark extract are responsible for the reduction and stabilization of the BAgNPs. The morphology and crystalline phase of the nanocrystals were determined by TEM and XRD. The hydrodynamic diameter (96.8nm) and a negative zeta potential (-14.6mV) were measured using the dynamic light scattering technique. The antimicrobial activity of AgNPs was evaluated (in vitro) against fungi, bacteria using disc diffusion method which were isolated from the scales formed in drinking water PVC pipelines. MTT assay studied by HepG2 cell lines showed significant cytotoxic activity with IC50 value. In, the present study nanoparticles shown very good Antibiofilm activity towards fungi and bacteria isolated from PVC pipeline biofilm and these types of nanoparticles will show major challenge is designing particles that have long circulation times and low toxicity. Herein, we suggest green synthesis of AgNPs with potent antibacterial, antifungal, and anti-scaling activities with feasible biomedical and industrial applications and the scope for further development of anticancer drugs.

Keywords: Biogenic Ag nanoparticles; Anti-fungal activity; Anti-bacterial activity; stem bark extract of *Boswellia ovalifoliolata*; HepG2 cell lines

1. Introduction

Nanoparticles, generally considered as particles with a size of up to 100 nm, exhibit completely new or improved properties as compared to the larger particles of the bulk material that they are composed of based on specific characteristics such as size, distribution, and morphology.^[1] Nanoparticles of noble metals, such as gold, silver, and platinum, are widely applied in products that directly come in contact with the human body, such as shampoos, soaps, detergent, shoes, cosmetic products, and toothpaste, besides medical and pharmaceutical applications. Therefore, there is a growing need to develop environmentally friendly processes for nanoparticle synthesis without using toxic chemicals. Biological methods for nanoparticle synthesis using microorganisms, enzymes, and plants or plant extracts have been suggested as possible ecofriendly alternatives to chemical and physical methods.^[2] There have been recent reports on phytosynthesis of silver and gold nanoparticles by

employing coriander leaves,^[3] sundried Cinnamomum camphora leaves,^[4] phyllanthin extract,^[5] purified apiin compound extracted from henna leaves,^[6] Citrus reticulata^[7] and Dioscorea batatas [8]. *Boswellia ovalifoliolata* Bal & Henry is a narrow endemic, endangered and threatened medicinal tree species. It is deciduous medium sized tree belongs to the family Burseraceae. This tree harbours on Tirumala hills of Seshachalam hill range of Eastern Ghats of India.

The plant is used by tribals like Nakkala, Sugali and Chenchu and indigenous community to treat number of ailments. The plant is over exploited for its medicinal uses; especially the stem bark is used to reduce rheumatic pains.^[9] Stem bark decoction is given orally to reduce the pains. Equal mixture of Gum & Stem bark one tea spoon full given daily with sour milk an empty stomach for a month to cure stomach ulcers.^[10] Although this plant is considered as undesirable plant, Silver nanoparticles are widely used for its unique properties in catalysis, chemical sensing, biosensing, photonics, electronic and pharmaceuticals and in biomedicine especially for antibacterial agent

and antiviral agent. Silver nanoparticles have a great potential for use in biological including antimicrobial activity. Antimicrobial capability of silver nanoparticles allows them to be suitably employed in numerous household products such as textiles, food storage containers, home appliances and in medical devices. Silver is an effective antimicrobial agent exhibits low toxicity. The antibacterial and antifungal activity of silver species has been well known since ancient times. The most important application of silver and silver nanoparticles is in medical industry such as tropical ointments to prevent infection against burn and open wounds. Biologic synthesis of nanoparticles by plant extracts is at present under exploitation as some researchers worked on it and testing for antimicrobial activities. However, hardly reports are available on antimicrobial activity of silver nanoparticles synthesized using the aqueous extract of this plant. Therefore, in the present investigation, we have synthesized AgNPs using the aqueous stem bark extract of *Boswellia ovalifoliolata* and evaluated the antimicrobial efficacy of as prepared AgNPs against pathogenic fungi and bacteria (Biofilm degradation in drinking water pipelines) using disc diffusion (in-vitro) method.

2. Materials and measurements methods

Silver nitrate (>99% pure) was purchased from Sigma Aldrich, India. Potato dextrose broth, Potato dextrose agar, Nutrient broth, Nutrient agar plate, was supplied by Hi-media, India.

2.1. Collection of biofilm formed in poly vinyl chloride (PVC) pipes

The PVC Biofilm samples were collected from four different regions located in and around Tirupati, (Chittoor District) Andhra Pradesh, India. The samples were collected from drinking water PVC pipelines and taken in the sterile container. These samples were stored in an ice box and transported to the laboratory for microbiological characterization.

2.2. Collection of Plant Material

Healthy *Boswellia ovalifoliolata* stem barks were collected from Tirumala hills, Andhra Pradesh state, India. From the selected plant bark was collected by scrapping the trunk using neat and clean knife during the month of June 2016 and collected material was carefully washed and dried at 45°C to constant weight. The dried bark of plant material were powdered, passed through a BSS no. 85-mesh sieve and stored in air tight container.

2.3. Preparation of aqueous bark extract

The collected *B. ovalifoliolata* stem bark was allowed to shade dried for 72 h and was ground to get fine powder. Then, 10 g of powder was mixed with 100mL of distilled water and boiled for 30 min. After that, the extract was filtered by using Whatman No. 1 filter paper and collected the filtrate in plastic bottle and stored at 4°C for further characterization and experimentation.

2.4. Isolation of fungal and bacterial sp. from drinking water pipeline

Eight fungal species and ten bacterial samples were isolated from drinking water supply PVC pipelines in Tirupati, Chittoor district, AP,

India. Through serial dilution pour plate technique, fungal sp. was isolated using potato dextrose agar (PDA) medium and Gram-negative and Gram-positive bacteria were isolated from nutrient agar medium. Further, it is maintained in potato dextrose agar slants (fungi) and nutrient agar slants (bacteria) for onward analysis. Morphologically dissimilar colonies were selected randomly from all plates and isolated colonies were purified using appropriate medium by streaking methods. Extraction of DNA from Bacterial amplification by using PCR approximately 1300bp of a consensus 16S rRNA gene: forward primer 63f (51- CAG GCC TAA CAC ATG CAA GTC-3¹) and reverse primer 1387r (51- GGG CGG WGT GTA CAA GGC-3¹) Primers 27f and 1392r were also used and Fungal genomic DNA was extracted by using the CTAB fungal amplification by using PCR approximately 200-bp with primer ITS-1f (51- CAACTCCCAACCCCTGTGA-3¹) and reverse primer ITS-4r (51- GCGACGATTACCAGTAACGA-3¹). Then the pure cultures of bacterial and fungal species were sent to sequence analysis, raw sequences were edited and assembled using the Auto Assembler program (V5.2). All the sequences were used to identify the bacteria and fungi with the help of the BLASTn program <http://www.ncbi.nlm.nih.gov/BLAST>.

2.5. Preparation of *Boswellia ovalifoliolata* Silver nanoparticles

To prepare the BAgNPs, a 90-mL aqueous solution of 1.0×10^{-3} M silver nitrate was mixed with a 10-mL of 5% aqueous solution of *Boswellia ovalifoliolata* bark extract. The *Boswellia ovalifoliolata* Ag solution was yellow in color and the solution was stirred repeatedly for an hour and observed that the color of the solution has been changed to dark brown which visually confirms the formation of nanoparticles. The initial concentration of the *Boswellia ovalifoliolata* silver nanoparticles was measured using ICP-OES and was found to be 170ppm. Then, by diluting this solution, each sample of different concentration was used to investigate the concentration dependence of the antibacterial effect of Ag nanoparticles. This *Boswellia ovalifoliolata* silver nanoparticles was characterized by using the techniques like, X-ray diffractometry (XRD), Fourier transform infrared spectrophotometry, (FTIR), UV-Vis spectrophotometry, Dynamic light scattering (Particle size), zeta potential and Transition electron microscopy (TEM).

2.6. Measurement of concentration of BAgNPs using inductively coupled plasma optical emission spectrophotometer (ICP-OES)

The concentrations of the *Boswellia ovalifoliolata* bark extract mediated AgNPs were measured using inductively coupled plasma optical emission spectrophotometer (ICP-OES) (Prodigy XP, Leeman labs, USA). The samples were prepared with 10 times dilution after centrifugation at 4000 rpm for 15 min. Then 20ml of aliquot was loaded to the racks of automatic sampler and estimated the concentration of AgNPs thrice.

2.7. Anticancer activity of *Boswellia ovalifoliolata* produced AgNPs using human hepatic carcinoma (HepG2) cell line and treatment procedure

The human hepatic carcinoma cell line (HepG2) was obtained from National Centre for Cell Science (NCCS), Pune, India and grown in

Eagles Minimum Essential Medium containing 10% fetal bovine serum (FBS). The cells were maintained at 5% CO₂ and incubated at 37°C for 24 hours. After 24h the cells were treated with serial concentrations of the test sample (Ag nanoparticles) (5, 15, 25, 50, and 100 µg/ml) and placed in the humidified 5% CO₂ incubator for 48h. Cells incubated in culture medium alone served as a control for cell viability (untreated wells). Each experiment was repeated at least three times. After Ag nanoparticles treatment, cells were aspirated by 600 µL of phosphate buffer saline (PBS) (pH 7.0) and centrifuged for 20 min at 4000 rpm to remove cell debris and obtain a clear supernatant.

2.8. MTT assay

The MTT assay is a colorimetric assay for measuring the activity of cellular enzymes that reduce the tetrazolium dye, MTT, to its insoluble formazan, giving a purple color. MTT (3-(4,5 dimethylthiazol-2-yl)-2,5-diphenyltetrazolium bromide, a yellow tetrazole), is reduced to purple formazan in living cells. After 48h of incubation, 10µl of MTT (5 mg/ml) in phosphate buffered saline (PBS) was added to each well and incubated at 37°C for 5 h. The medium with MTT was then flicked off and the formed formazan crystals were solubilized in 100 µl of DMSO and then measured the absorbance at 570 nm using micro plate reader. The percentage cell viability was then calculated with respect to control as follows

$$\% \text{ Cell viability} = [A] \text{ Test} / [A] \text{ control} \times 100$$

2.9. Assay for antimicrobial activity of *Boswellia ovalifoliolata* silver nanoparticles against microorganisms (Fungi and Bacteria)

The antimicrobial activity of *Boswellia ovalifoliolata* silver nanoparticles was examined on the basis of colony formation by in vitro Petri dish assays (Disc diffusion). Each fungal and bacterial isolate was cultured on growth media that induced prolific conidia and bacterial production. The fungus isolates were grown on potato dextrose agar medium and bacterial isolates were grown on nutrient agar medium. Conidia were collected from cultures that were incubated at 37°C for 10 days (Fungi) and Bacterial cultures were collected from cultures that were incubated at 37°C for 2 days for (Bacteria), and diluted with sterile, deionized water to a concentration of 10⁶ spores' ml⁻¹. Aliquots of the conidial suspension and bacterial suspension were mixed with serial concentrations of silver preparations to a final volume of 1 ml and were also mixed with sterile, deionized water as control. A 10-µl subsample of the conidia and *Boswellia ovalifoliolata* silver mixture stock was taken at 50±0.9ppm, 100±1.1ppm and 170±1.4ppm after silver treatments and diluted 100-fold with the deionized water. A 10-µl aliquot of the diluted spore suspension was spread on potato dextrose agar (PDA; Becton, Dickson and Company, Sparks, MD) medium. Three PDA plates for fungi and three NA plates for bacteria per each combination of exposure *Boswellia ovalifoliolata* silver concentration were tested. The filter paper disc dipped in different ppm and inserted on mediums (PDA) then the plates were incubated at 37°C for 2-4 days for fungi and bacteria respectively. The average number of colonies from silver-treated spore suspensions (fungi) and (bacteria) was compared with the number on the water control

(percent colony formation). The zone size was determined by measuring the diameter of the zone in mm.^[11-13]

2.10. Characterization of silver nanoparticles

2.10.1. UV – Visible spectrum for synthesized nanoparticles

The bio-reductant nanoparticles were monitored by UV–visible spectrum at various time intervals. The UV – Visible spectra of this solution was recorded in spectra 2450, SHIMADZU Spectrophotometer, from 400 to 800 nm.

2.10.2. FTIR Analysis for synthesized nanoparticles

The FTIR spectrum was taken in the mid IR region of 400–4000 cm⁻¹. The spectrum was recorded using ATR (attenuated total reflectance) technique. The dried sample was mixed with the KBr (1:200) crystal and the spectrum was recorded in the transmittance mode.

2.10.3. Particle Size and Zeta potential analyzer for synthesized nanoparticles

The aqueous suspension of the synthesized nanoparticles was filtered through a 0.22 µm syringe driven filter unit and the size and distribution of the nanoparticles were measured using Dynamic Light Scattering (DLS) technique (Nanopartica, HORIBA, SZ-100).

2.10.4. X-ray Diffraction (XRD) analysis for synthesized nanoparticles

The phyto-reduced silver nanoparticles were characterized by XRD. The XRD pattern was recorded using computer controlled XRD-system (JEOL, and Model: JPX-8030 with CuKα radiation (Ni filtered = 13418 Ao) in the range of 40kV, 20A. The built in software (syn master 7935) program was used for the identification of XRD peaks corresponds to the Bragg's reflections.

2.10.5. Transmission Electron Microscopy (TEM)

The surface morphology and size of the nanoparticles was studied by Transmission electron microscopy (JEOL (JEM-1010) instrument) with an accelerating voltage of 80 kV. A drop of aqueous AgNPs on the carbon-coated copper TEM grids were dried and kept under vacuum in desiccators before loading them onto a specimen holder. The particle size and surface morphology of nanoparticles was evaluated using ImageJ 1.45s software.

2.10.6. Laser Raman spectroscopy

A Raman spectrophotometer is to detect the maximum sensitivity of the product. The surface defects and sp² hybridization of grapheme sheets were determined by LASER RAMAN spectroscopy (RFS 100/S-Bruker, Inc., Karlsruhe, Germany, Matlab 6.0 software) at the excitation wavelength of 633 nm with exposure time of 10 s (100% intensity).



Fig. 1. *Boswellia ovalifoliolata* Stem Bark and bark powder.

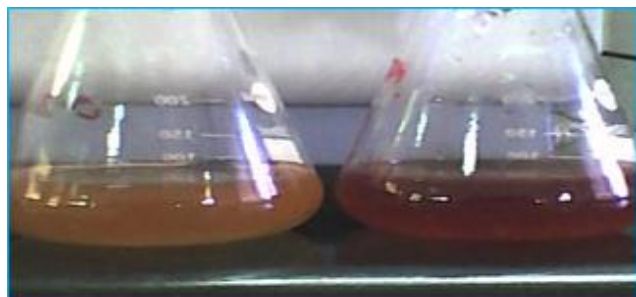


Fig. 2. Color change of 1mM AgNO₃ solution before and after addition of *B. ovalifoliolata* bark extract (color changes from light brown to dark brown color)

2.11. Statistical analysis

All of the data from three independent replicate trials were subjected to analysis using Statistical package for the Social Sciences (SPSS) version 16.0. The data are reported as the mean \pm SD and significant differences between mean values were determined with one way analysis of variance (CRD) followed by Duncan's multiple range test (DMRT) ($P \leq 0.05$).

3. Results and Discussions

3.1. Selection of fungi and bacteria present in drinking water pipeline and synthesis of silver nanoparticles

Drinking water pipeline fungi and bacterial species have unusual biological activities depending upon the metabolisms under temperature, pH and pressure. Once, the bark (Fig. 1) extract (10ml) was treated with 90ml of silver nitrate solution, the color of the solution changed to dark brown color (Fig. 2) in less than 5 minutes. The brown color was primarily due to the surface Plasmon resonance of the formed silver nanoparticles.

3.2. UV-Visible spectral analysis – Recording of localized surface plasmon resonance (LSPR) of AgNPs

UV-Visible spectroscopy was employed to understand the biosynthesis of silver nanoparticles by *Boswellia ovalifoliolata* (Fig. 3) shows the UV-Visible adsorption spectra of silver nanoparticles after 24hrs incubation at room temperatures (37°C). The spectrum shows peaks at 410–460 nm. But the maximum absorbance peak is observed at 430nm under 37°C in 24 hrs; the short time enough for the silver ions to silver nanoparticles at 37°C temperature. Silver reduction capacity was observed under UV-Visible adsorption spectroscopy.

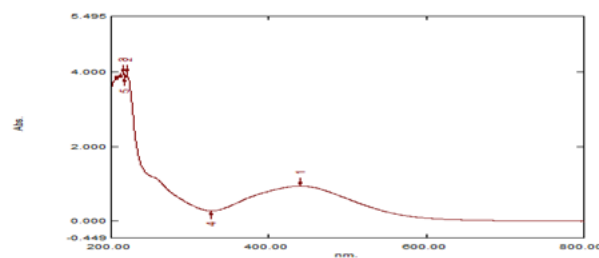


Fig. 3. UV-visible spectroscopic micrograph showing the localized surface plasmon resonance (LSPR) of Ag nanoparticles synthesized using *Boswellia ovalifoliolata* stem bark extract.

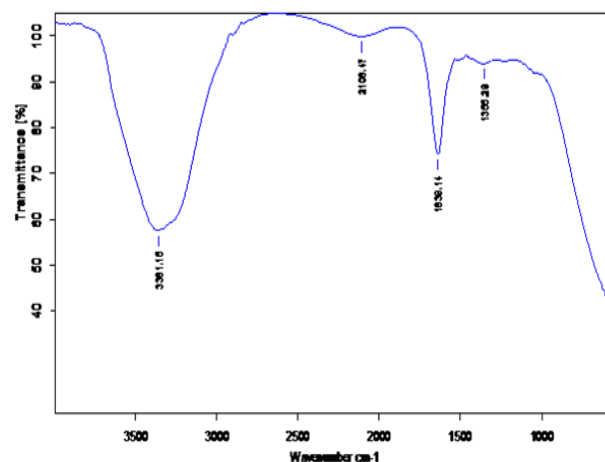


Fig. 4. FT-IR spectroscopic micrograph showing the functional groups responsible for the reduction and stabilization of Ag nanoparticles synthesized using the aqueous extract of *Boswellia ovalifoliolata* stem bark.

This shows UV-Vis spectra obtained from solution at room temperature at 7.0 pH. The overall observations suggest that the bio reduction of (silver ions) Ag⁺ to Ag (0) was confirmed by UV-Visible spectroscopy UV-Vis spectrograph of the colloidal solution of silver nanoparticles has been recorded as a function of time. Absorption spectra of silver nanoparticles formed in the reaction media at 10 min. has absorbance peak at 430 nm, broadening of peak indicated that the particles are poly dispersed. The bio-reduction of aqueous Ag⁺ ions by the stem bark extract of the plant *Boswellia ovalifoliolata* has been demonstrated. The reduction of the metal ions through bark extracts leading to the formation of silver nanoparticles of fairly well-defined dimensions.

3.3. FT-IR analysis – Identification of the biomolecules responsible for the reduction and stabilization of AgNPs

FT-IR spectrum is used to identify the possible chemical interactions among the silver salts and functional groups present in cell filtrate. FT-IR spectrum of the biosynthesized silver nanoparticles using *Boswellia ovalifoliolata* (Fig. 4) shows the absorption peaks at 1414.78, 1640, 2108.51, 3380 cm⁻¹ and 568 cm⁻¹. The peak at 3380 and 2018.5 cm⁻¹ reveals the presence of N-H bend, indicating the primary and secondary amine groups of protein. Likewise, the bands at 1,640 and 1414.78 cm⁻¹ correspond to the primary and secondary amine groups of N-H bending and carbonyl stretching vibrations of protein, the peak present at 568 cm⁻¹ shows stretching vibration of

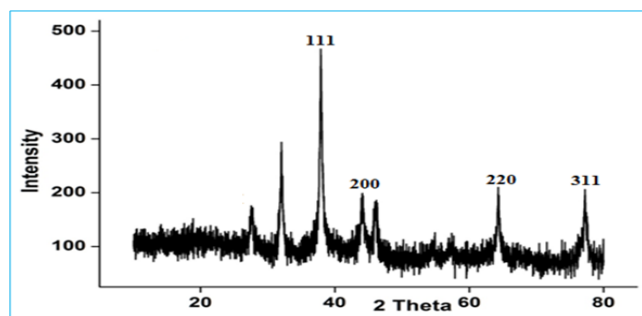


Fig. 5. XRD pattern of capped silver nanoparticles synthesized using *Boswellia ovalifoliolata* stem bark.

C-Br group respectively indicating the involvement of proteins in reduction and stabilization of silver ions. The FTIR study has shown that the carbonyl group of amino acid residues and peptides of proteins has a stronger metal-binding capability. Most possibly, the proteins could form a coat to cover the nanoparticles and act as capping agents for silver nanoparticle formation to avert the agglomeration of the nanoparticles; therefore, the particles are stabilized.^[14] The FT-IR observations indicate that the bio-reductions of silver nitrate are tied to the oxidation of hydroxyl groups in fungal cell filtrate.^[15]

3.4. X-Ray Diffraction (XRD) analysis

XRD confirming the existence of silver colloids in the sample. The Bragg reflections were observed in the XRD pattern at $2\theta = 32.4$, 46.4 and 28.0 . These Bragg reflections clearly indicated the presence of (111), (200), (220) and (311) sets of lattice planes and further on the basis that they can be indexed as face-centered-cubic (FCC) structure of silver (Fig. 5). Hence XRD pattern thus clearly illustrated that the silver nanoparticles formed in this present synthesis are crystalline in nature. In addition to the Bragg peaks representative of FCC silver nanoparticles, additional as yet unassigned peaks were also observed suggesting that the crystallization of bioorganic phase occurred on the surface of the nanoparticles. The crystalline size was calculated from the width of the peaks present in the XRD pattern, assuming that they are free from non-uniform strains, using the Debye-Scherrer formula.

$$D = 0.94 \lambda / \beta \cos \theta$$

Where D is the average crystalline domain size perpendicular to the reflecting planes; λ (1.5406×10^{-10}) is the X-ray wavelength used; β is the full width at half maximum (FWHM) and θ is the diffraction angle.^[16] The calculated crystalline size of the AgNPs was 100nm.

3.5. Dynamic light scattering analysis

Particle size and zeta potential values were measured using Nanopartica SZ-100. The particle size distribution spectra for the silver nanoparticles were recorded as diameter (nm) versus frequency (%/nm) spectra with diameter (nm) on x-axis and frequency (%/nm) on y-axis. The zeta potential spectra for the silver nanoparticles were recorded zeta potential versus intensity spectra with zeta potential (mV) on x-axis and intensity (a.u) on y-axis.

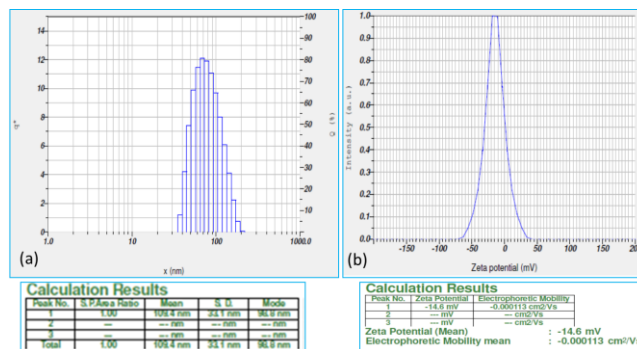


Fig. 6(a, b). Showing the histogram of silver nanoparticles (Dynamic light scattering) and zeta potential (-14.6mV) of Silver nanoparticles synthesized using the stem bark extract of *Boswellia ovalifoliolata*.

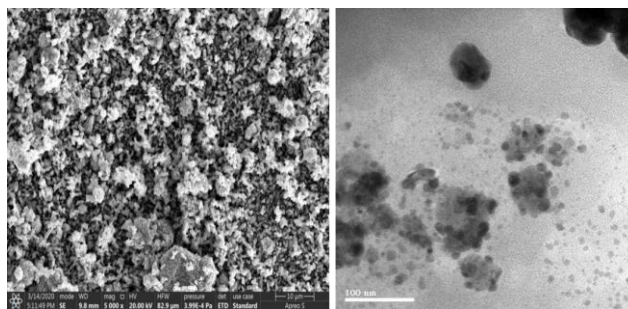


Fig. 7. SEM and TEM image of *Boswellia ovalifoliolata* stem bark silver nanoparticles showing spherical shaped particles with an average size of 100nm.

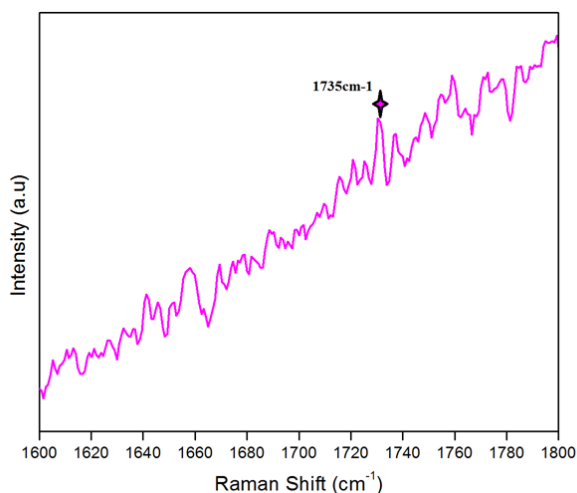
Particle size of 96.8 nm with zeta potential of -14.6mV was recorded for the silver nanoparticles synthesized from *Boswellia ovalifoliolata* bark extract (Fig. 6a and 6b). In DLS signifies the presence of repulsive electro-static forces among the synthesized silver nanoparticles, which leads to the monodispersity of the particles. If the hydrosol has a large negative or positive zeta potential then they will tend to repel with each other and there will be no tendency of the particles to agglomerate. The zeta potential indicates the degree of repulsion between adjacent and similarly charged particles in dispersion. For the silver nanoparticles synthesized from *Boswellia ovalifoliolata* bark extract, high particle size and less zeta potential values were recorded. The zeta potential value indicated good stability with high potential. Particle size is measured by the SZ-100 using dynamic light scattering (DLS). However, if the particles have low Zeta potential values then there will be no force to prevent the particles coming together and flocculating.

3.6. SEM and TEM analysis

The micrographs of Scanning electron microscopy and Transmission Electron Microscopy have provided further insight into the morphology and size details of the silver nanoparticles. The representative SEM and TEM picture recorded from the silver nanoparticles film deposited on a carbon coated copper TEM grid shown in (Fig. 7). TEM picture shows individual silver nanoparticles as well as a number of aggregates due to the absence of surface protecting ligands and it is spherical in shape. The particles were crystalline in nature as revealed by the high magnification TEM image

Table 1. Cytotoxic activity of *Boswellia ovalifoliolata* stem bark extract mediated synthesized AgNPs against Human hepatic carcinoma cell line (HepG2)

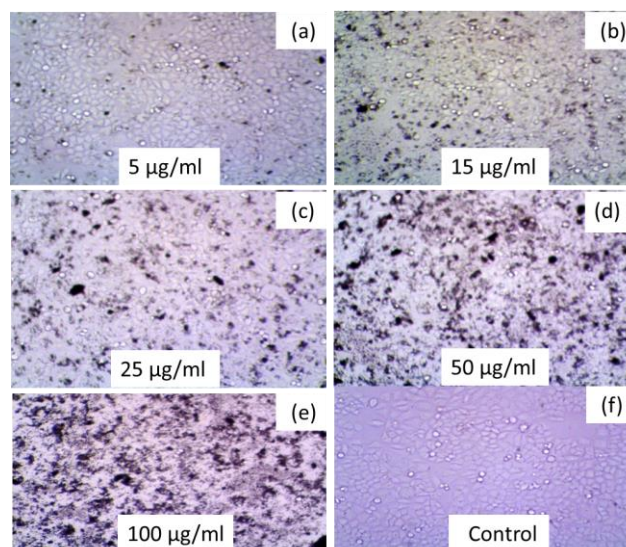
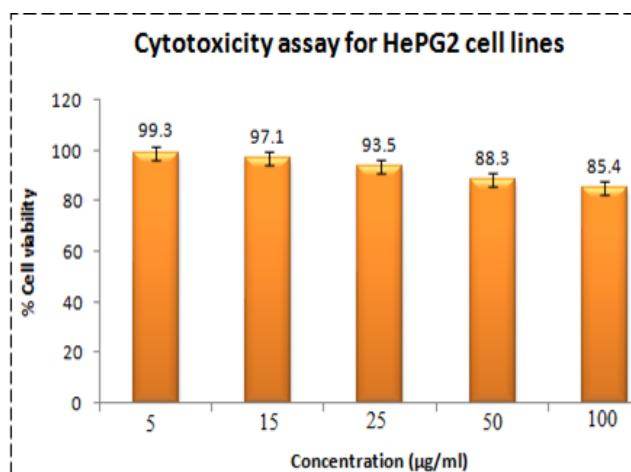
S. No	Concentration ($\mu\text{g/ml}$)	% Cell viability
1	5	99.3
2	15	97.1
3	25	93.5
4	50	88.3
5	100	85.4

**Fig. 8.** Laser Raman spectroscopic analysis of *Boswellia ovalifoliolata* stem bark extract mediated Synthesis of silver nanoparticles.

of nanoparticles and the lattice of silver was clearly seen. In general particles were spherical in shape and the sizes of the silver nanoparticles were found in the range of 100nm in TEM where as in SEM it is 10 μm .

3.7. Laser Raman spectral analysis

We have ensured that the concentration of Ag nanoparticles used in our study was kept sufficiently low to preclude auto-oxidation induced by surface-enhanced Raman effects. This is made evident in the spectra we present in the following: there is no enhancement observed in the overall strength of the Raman signal that is obtained from our nanoparticle, The highest peak was seen in 1735 cm^{-1} Indicating C-N stretching vibrations seen in (Fig. 8). The Raman spectrum shows prominent vibration band related to silver nanoparticles shows the major peak, raised from 1735 cm^{-1} , which shows the presence of silver and very small disturbance of the peaks seen around the major peak is due to proteins present in *Boswellia ovalifoliolata* stem bark extract, There are inconsistent variations in the relative intensities of several other vibration bands, and we could not find any concrete link with specific biochemical modifications. It has been reported that the exposure of Ag nanoparticles may lead to an increase in ROS (reactive oxygen species) and cell death, indicating that the mechanism of NP-induced cytotoxicity may be through oxidative stress, It has been well recognized that free radicals are frequently generated upon introduction of diverse nanomaterials, and such free radicals play an important role in generating NP-induced toxicity. Our results appear to be in consonance with what has been established in a general context in several earlier studies.

**Fig. 9.** Human hepatic carcinoma cell line (HepG2) treated with 5–100 $\mu\text{g/ml}$ of Synthesized by AgNPs using *Boswellia ovalifoliolata* stem bark extract (a) 5 μg (b) 15 μg (c) 25 μg (d) 50 μg (e) 100 μg (f) Control.**Fig. 10.** Cytotoxic activity of Human hepatic carcinoma cell line (HepG2) Synthesized by AgNPs using *Boswellia ovalifoliolata* stem bark extract.

3.8. MTT Assay

The in-vitro cytotoxic effects of AgNPs were screened against HepG2 cell line and the percentage of cell inhibition was confirmed by MTT assay (Table 1). After 48 h of treatment, the AgNPs at concentration of 5 $\mu\text{g/ml}$ shown 99.3 viability, 15 $\mu\text{g/ml}$ shown 97.1, 25 $\mu\text{g/ml}$ shown 93.5, 50 $\mu\text{g/ml}$ shown 88.3 and 100 $\mu\text{g/ml}$ shown 85.4 of viability of HepG2 cells, and this was chosen as IC50 (Fig. 9 & 10). The cytotoxic effects of AgNPs are the active physico-chemical interaction of silver atoms with the functional groups of intracellular proteins, nitrogen bases and phosphate groups in DNA. Although, further studies are needed to fully understanding the mechanism involved in the anticancer activity. From our results, it can be concluded that the *Boswellia ovalifoliolata* nanoparticles could have induced intracellular reactive oxygen species generation, which can be evaluated using intracellular peroxide-dependent oxidation and caused cell death slightly. The control cells were clustered, healthy and viable cells the *Boswellia ovalifoliolata* silver nanoparticles

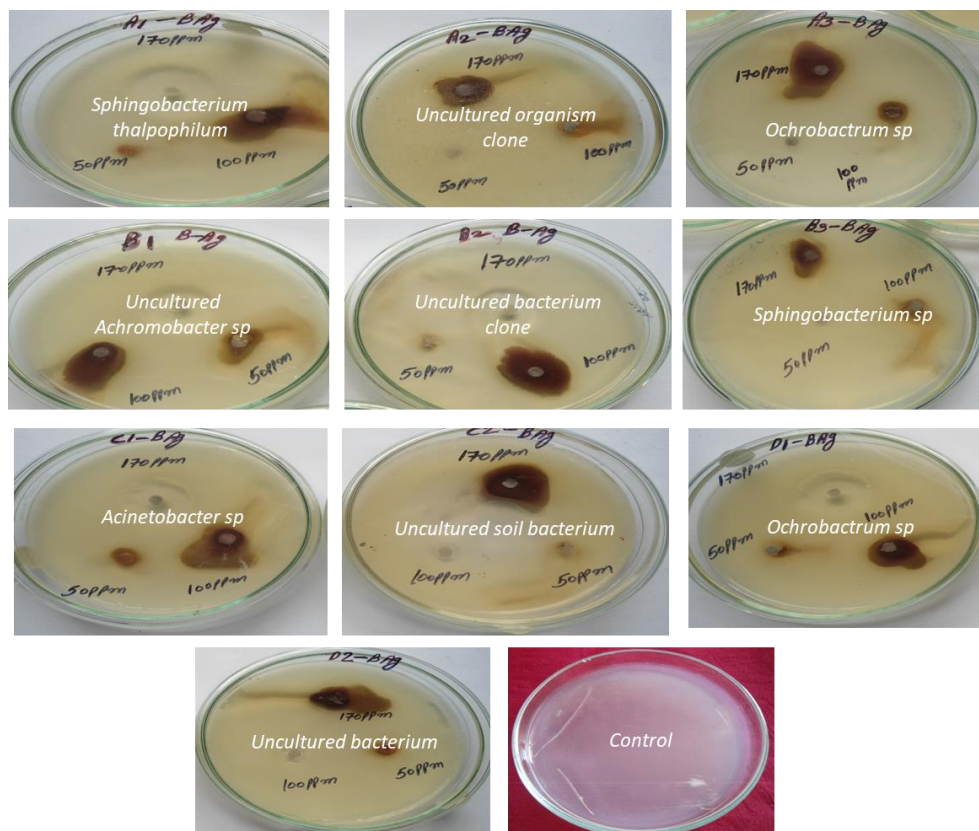


Fig. 11. Antibacterial activity of *Boswellia ovalifoliolata* stem bark extract mediated silver nanoparticles against Gram positive and Gram negative bacteria (Plate 1).

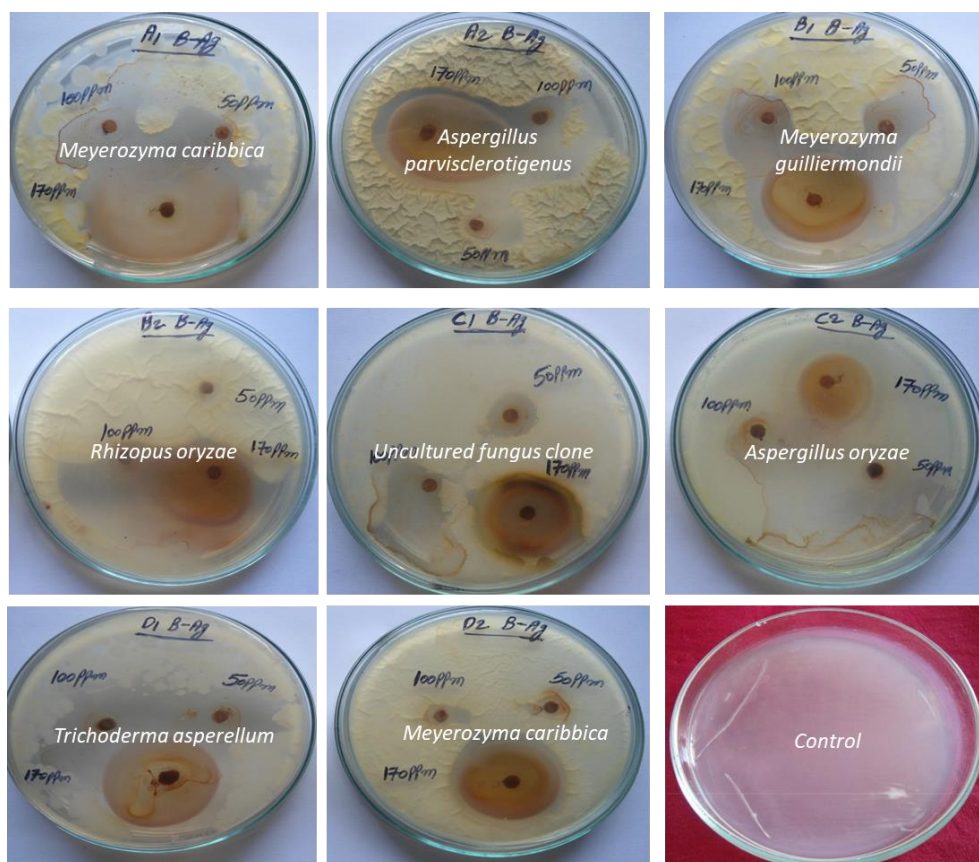


Fig. 12. Antibacterial activity of *Boswellia ovalifoliolata* stem bark extract mediated silver nanoparticles against Fungal sp isolated from drinking water PVC pipelines (Plate 2).

Table 2. *In-vitro* antibacterial studies of bacteria present in drinking water PVC pipelines using *Boswellia ovalifoliolata* silver nanoparticles as inhibitors

S. no	Bacteria	<i>Boswellia ovalifoliolata</i> stem bark extract mediated synthesis of silver nanoparticles Zone of inhibition (mm)		
		170±1.4ppm	100±1.1ppm	50±0.9ppm
1.	<i>Sphingobacterium thalpophilum</i>	2.4±0.05 ^a	1.5±0.02 ^c	1.0±0.02 ^a
2.	<i>Uncultured organism clone</i>	2.8±0.06 ^a	2.0±0.02 ^{ab}	1.5±0.04 ^a
3.	<i>Ochrobactrum sp</i>	2.0±0.07 ^{cdef}	1.1±0.02 ^{de}	0.5±0.16 ^{de}
4.	<i>Uncultured Achromobacter sp</i>	2.1±0.17 ^{cdef}	1.8±0.02 ^b	1.2±0.06 ^a
5.	<i>Uncultured bacterium clone</i>	2.2±0.14 ^{abc}	1.2±0.02 ^d	0.9±0.05 ^{ab}
6.	<i>Sphingobacterium sp</i>	1.5±0.19 ^g	1.0±0.02 ^{def}	0.5±0.12 ^{def}
7.	<i>Acinetobacter sp</i>	2.2±0.12 ^{abcd}	2.1±0.02 ^a	1.0±0.08 ^{ab}
8.	<i>Uncultured soil bacterium</i>	2.4±0.08 ^{ab}	0.9±0.02 ^{efg}	0.5±0.17 ^{def}
9.	<i>Ochrobactrum sp</i>	2.2±0.06 ^{abcde}	1.5±0.02 ^c	0.6±0.08 ^{cd}
10.	<i>Uncultured bacterium</i>	1.7±0.07 ^g	0.8±0.02 ^{fg}	0.7±0.07 ^c
C.R.D (P≤0.05)		0.227	0.220	0.156

Data followed by the same letter are not significantly different at P≤0.05, whereas those followed by different letters are significantly different at P≤0.05.

Table 3. *In-vitro* antifungal studies of fungi present in drinking water PVC pipelines using *Boswellia ovalifoliolata* Silver nanoparticles as inhibitors

S. no	Fungi	<i>Boswellia ovalifoliolata</i> stem bark extract mediated synthesis of silver nanoparticles Zone of inhibition (mm)		
		170±1.4ppm	100±1.1ppm	50±0.9ppm
1.	<i>Meyerozyma caribbica</i>	5.0±0.17 ^a	2.3±0.02 ^{de}	1.5±0.04 ^a
2.	<i>Aspergillus parvisclerotigenus</i>	3.5±0.06 ^{abcd}	1.7±0.01 ^f	1.4±0.08 ^{abc}
3.	<i>Meyerozyma guilliermondii</i>	3.8±0.03 ^{ab}	2.1±0.08 ^e	2.0±0.04 ^a
4.	<i>Rhizopus oryzae</i>	4.0±0.05 ^a	3.0±0.04 ^a	1.0±0.03 ^d
5.	<i>Uncultured fungus clone</i>	2.6±0.04 ^a	1.5±0.05 ^f	1.3±0.04 ^{abc}
6.	<i>Aspergillus oryzae</i>	3.2±0.09 ^{cde}	2.7±0.16 ^{ab}	1.5±0.02 ^{ab}
7.	<i>Trichoderma asperellum</i>	3.5±0.04 ^{abcde}	2.7±0.27 ^{abc}	0.5±0.09 ^{de}
8.	<i>Meyerozyma caribbica</i>	3.7±0.06 ^{abc}	2.5±0.08 ^{bcd}	1.0±0.06 ^d
C.R.D (P≤0.05)		0.514	0.356	0.281

Data followed by the same letter are not significantly different at P≤0.05, whereas those followed by different letters are significantly different at P≤0.05

treated cells showed slightly increased apoptosis morphological changes also the clearly visible cell debris is due to cell death at dose of 15 µg/ml silver nanoparticles treatment. Further studies have to be carried out to understand the nature of cytotoxicity and the death or proliferation of cells caused by *Boswellia ovalifoliolata* extract mediated silver nanoparticles.

The silver nanoparticles were biologically synthesized from *Boswellia ovalifoliolata* extract and the method proved to be economical and environmentally benign. These well-defined phylogenetic silver nanoparticles showed enhanced antimicrobial properties against an array of bacterial and fungal species. The previous *in vitro* cytotoxic studies proved that Ag-NPs have dose-dependent cytotoxic effects on human liver HepG2 cells due to trigger of oxidative stress and induction of apoptosis, mediated by mitochondrial injury via the generation of reactive oxygen species or increases in intracellular oxidative stress and trigger cell death process including apoptosis and necrosis.

The anticancer effect of silver nanoparticles against HepG2 lines was performed the results show the good cytotoxic activity against the cancer cells. The concentration of silver nanoparticles plays an important role in the anticancer activity. The silver nanoparticles are having the good results followed by 5 µg/ml, 15 µg/ml, 25 µg/ml, 50 µg/ml and 100 µg/ml. The lowest inhibitory action was observed from the concentration of 100 µg/ml. Our study describes the potential use of *Boswellia ovalifoliolata* as a source of anti-cancer drug.

The nature of plant extract directly affects the physical, chemical and cytotoxic properties of the nanoparticles due to the interaction

of nanoparticles with cells and intracellular macromolecules like proteins and DNA. Cell damage by silver nanoparticles may be due to loss of cell membrane integrity, apoptosis and oxidative stress. The anticancer activity was observed and that the synthesized silver nanoparticles induce a dose dependant inhibition activity against HepG2 cells. Some of the approved chemotherapeutic agents were caused side effect and high cost. Therefore there is an important need to develop alternative medicines against this deadly disease. Biosynthesis of silver nanoparticles using *Boswellia ovalifoliolata* extract was developed in a very simple and eco-friendly method. Generally, plants containing proteins have played a major role in acting as a reductant as well as a capping material in order to synthesize AgNPs that functioned effectively as an anticancer agent against HepG2 cancer cells.^[19]

3.9. Antimicrobial efficacy of *Boswellia ovalifoliolata* bark extract mediated silver nanoparticles

BAGNPs have very strong inhibitory action against fungal sp, Gram-positive and Gram-negative bacteria (Plate 1 (Fig. 11) and Plate 2 (Fig. 12)). Three concentrations of BAGNPs (170, 100, 50ppm) were prepared and were applied against an array of fungal species viz., *Meyerozyma caribbica*, *Aspergillus parvisclerotigenus*, *Meyerozyma guilliermondii*, *Rhizopus oryzae*, *Uncultured fungus clone*, *Aspergillus oryzae*, *Trichoderma asperellum* and bacterial species viz., *Sphingobacterium thalpophilum*, *Uncultured organism clone*, *Ochrobactrum sp*, *Uncultured Achromobacter sp*, *Uncultured bacterium clone*, *Sphingobacterium sp*, *Acinetobacter sp*, *Uncultured*

soil bacterium, *Ochrobactrum sp.* which were isolated from drinking water PVC pipes. The higher concentration (170ppm) of AgNPs showed significant antimicrobial effect (Tables 2 and 3) compared with other concentrations (100, 50ppm). In a recent study of *Boswellia ovalifoliolata* complex slowly grows by further aggregation it reaches an optimal size at which stage the strong repelling layer prevents further aggregation. Further growth of these particles occurs via Ostwald ripening^[17] in which larger particles grow at the expense of smaller ones. As the smaller particles are oxidized, the Ag⁺ ions readsorb on the larger silver crystallites and undergo reduction at the metal surface. Such a reduction of Ag⁺ ions at the silver surface is facilitated by the decrease in the reduction potential at the metal surface compared to the bulk solution. A detailed mechanism on the preferential reduction of metal ions at the preformed metal crystallites has been established in earlier studies.

The mechanism of inhibitory action of silver ions on microorganisms is partially known. It is believed that DNA loses its replication ability and cellular proteins become inactivated on Ag⁺ treatment.^[18] In addition, it was also shown that Ag⁺ binds to functional groups of proteins, resulting in protein denaturation. The obvious question is how nanosize silver particles act as biocidal material against There are reports in the literature that show that electrostatic attraction between negatively charged bacterial cells and positively charged nanoparticles is crucial for the activity of nanoparticles as bactericidal materials.^[20-21] However, silver particles used in this study are negatively charged.^[22] While the mechanism of the interaction between these particles and the constituents of the outer membrane of bacteria is unfortunately still unresolved, it would appear that, despite their negative surface charge, they somehow interact with “building elements” of the bacterial membrane, causing structural changes and degradation and finally, cell death. Indeed, the TEM analysis confirms the incorporation of silver nanoparticles into the membrane structure. A bacterial membrane with this morphology exhibits a significant increase in permeability, leaving the bacterial cells incapable of properly regulating transport through the plasma membrane and, finally, causing cell death. It is well known that the outer membrane of bacterial cells is predominantly constructed from tightly packed lipopolysaccharide (LPS) molecules, which provide an effective permeability barrier.^[23-24]

We may speculate that a similar mechanism causes the degradation of the membrane structure of bacteria's during treatment with *Boswellia ovalifoliolata* bark extract silver nanoparticles. Extensive investigations directed to better understanding of interaction between silver nanoparticles and bacterial components should shed light on the mode of action of this nanomaterial as a biocidal material. Nano-silver showed excellent apoptosis rate due to their smaller size and spherical morphology. The present study contributes a novel and alternate approach in cancer therapy. The novelty of the present research is that complete cell inhibition (99.3%) of HepG2 cell lines with plant mediated nano-silver particles is obtained with 5µg/mL Thus, our results show that *Boswellia ovalifoliolata* mediated AgNPs have proved to be potential for use as one of the cancer chemotherapeutic agents, Synthesis of metallic nanoparticles using green resources like *Boswellia ovalifoliolata* is a challenging alternative to chemical synthesis, since

this novel green synthesis is pollutant free and eco-friendly synthetic rote for silver nanoparticles. NPs size-dependence might affect the generation of reactive oxygen species in cellular materials and how NP-induced physiochemical alterations might be correlated with NP-toxicity, further studies are needed to optimize the mechanism of AgNPs on cancer cells.

4. Conclusions

The stem bark aqueous extract of *Boswellia ovalifoliolata* has been proved to be one of the potential bio-sources to synthesize silver nanoparticles.

- The formed AgNPs are highly stable and polydispersed with the mean size of 96nm. At higher concentrations (170 ppm), significant antimicrobial activity of AgNPs has been recorded against fungal sp. and Gram-positive and Gram-negative bacteria and points to the commercial use of these phyto-medicine-coated AgNPs in biomedical applications and agriculture as fungicides for the effective control of disease-causing pathogens.
- The present evaluation of the anti-fungal property therefore offers a scientific basis for the use of this plant as suitable anti-fungal and anti-bacterial agent against a range of pathogens but further investigation against the broader range of pathogens is certainly required to identify the active ingredients.
- Herein, aqueous extract of *Boswellia ovalifoliolata* was used to synthesize well defined silver nanoparticles and were triggered cell death in HepG2 through apoptosis.
- The prepared silver nanoparticles were also shown excellent antimicrobial properties against an array of microbes.

Acknowledgements

Research facilities provided by Acharya N G Ranga Agricultural University (ANGRAU) at Institute of Frontier Technology, Regional Agricultural Research Station and Tirupati were used to carry out part of this research work and authors acknowledge ANGRAU for the same.

Conflicts of Interest

The authors declare no conflict of interest.

References

- 1 Willems; van den Wildenberg. Road Map Report on Nanoparticles. Barcelona, Spain: W&W Espana sl, 2005. [\[Link\]](#)
- 2 Mohanpuria P.; Rana N.K.; Yadav S.K. Biosynthesis of Nanoparticles: Technological Concepts and Future Applications. *J. Nanopart. Res.*, 2008, **10**, 507-517. [\[CrossRef\]](#)
- 3 Narayanan K.B.; Sakthivel N. Coriander Leaf Mediated Biosynthesis of Gold Nanoparticles. *Mater. Lett.*, 2008, **62**, 4588-4590. [\[CrossRef\]](#)
- 4 Huang J.; Li Q.; Sun D.; Lu Y.; Su Y.; Yang X.; Wang H.; Wang Y.; Shao W.; He N.; Hong J. Biosynthesis of Silver and Gold Nanoparticles by Novel Sundried *Cinnamomum camphora* Leaf. *Nanotechnology*, 2007, **18**, 105104. [\[Link\]](#)

- 5 Kasthuri J.; Kathiravan K.; Rajendiran N. Phyllanthin-assisted Biosynthesis of Silver and Gold Nanoparticles: A Novel Biological Approach. *J. Nanopart. Res.*, 2009, **11**, 1075-1085. [[CrossRef](#)]
- 6 Kasthuri J.; Veerapandian S.; Rajendiran N. Biological Synthesis of Silver and Gold Nanoparticles using Apiin as Reducing Agent. *Colloids Surf. B: Biointerfaces*, 2009, **68**, 55-60. [[CrossRef](#)]
- 7 Kavitha K.S.; Baker S.; Rakshith D.; Kavitha H.U.; Yashwantha Rao H.C.; Harini B.P.; Satish S. Plants as Green Source Towards Synthesis of Nanoparticles. *Int. Res. J. Biol. Sci.*, 2013, **2**, 66-76. [[Link](#)]
- 8 Sreekanth T.V.M.; Nagajyothi P.C.; Supraja N.; Prasad T.N.V.K.V. Evaluation of the Antimicrobial Activity and Cytotoxicity of Phyto-genic Gold Nanoparticles. *Appl. Nanosci.*, 2015, **5**, 595-602. [[CrossRef](#)]
- 9 Savithramma N.; Venkateswarlu P.; Suhrulatha D.; Basha S.K.M.; Devi C.V.R. Studies of *Boswellia ovalifoliolata* bal. And Henry-an Endemic and Endangered Medicinal Plant. *Bioscan*, 2010, **5**, 359-362. [[Link](#)]
- 10 Nagaraju N.; Rao K.N. A Survey of Plant Crude Drugs of Rayalaseema, Andhra Pradesh, India. *J. Ethnopharmacol.*, 1990, **29**, 137-158. [[CrossRef](#)]
- 11 Girija S.; Balachandran Y.L.; Kandakumar J. Plants as Green Nanofactories: Application of Plant Biotechnology in Nanoparticle Synthesis-A Review. *Plant Cell Biotechnol. Mol. Biol.*, 2009, **10**, 79-86. [[Link](#)]
- 12 Reeves D.S.; Wise R.; Andrews J.M.; White L.O. Clinical Antimicrobial Assay, Oxford University Press, New York, USA, 1999. [[Link](#)]
- 13 Aneja K.R. *Experiments in Microbiology, Plant Pathology, Tissue Culture and Mushroom Production Technology*. New Age International Limited, 2001. [[Link](#)]
- 14 Vigneshwaran N.; Ashtaputre N.M.; Varadarajan P.V.; Nachane R.P.; Paralikar K.M.; Balasubramanya R.H. Biological Synthesis of Silver Nanoparticles using the Fungus *Aspergillus flavus*. *Mater. Lett.*, 2007, **61**, 1413-1418. [[CrossRef](#)]
- 15 Sanghi R.; Verma P. Biomimetic Synthesis and Characterisation of Protein Capped Silver Nanoparticles. *Biores. Technol.*, 2009, **100**, 501-504. [[CrossRef](#)]
- 16 NVKV Prasad T.; Subba Rao Kambala V.; Naidu R. A Critical Review on Biogenic Silver Nanoparticles and their Antimicrobial Activity. *Curr. Nanosci.*, 2011, **7**, 531-544. [[CrossRef](#)]
- 17 Bajpai V.K.; Rahman A.; Kang S.C. Chemical Composition and Inhibitory Parameters of Essential Oil and Extracts of *Nandina domestica* Thunb. to Control Food-borne Pathogenic and Spoilage Bacteria. *Int. J. Food Microbiol.*, 2008, **125**, 117-122. [[CrossRef](#)]
- 18 Jin R.; Cao Y.; Mirkin C.A.; Kelly K.L.; Schatz G.C.; Zheng J.G. Photoinduced Conversion of Silver Nanospheres to Nanoprisms. *Science*, 2001, **294**, 1901-1903. [[CrossRef](#)]
- 19 Supraja N.; Prasad T.N.V.K.V.; Soundariya M.; Babujanarthanam R. Synthesis, Characterization and Dose Dependent Antimicrobial and Anti-Cancerous Activity of Phycogenic Silver Nanoparticles against Human Hepatic Carcinoma (HepG2) Cell Line. *AIMS Bioeng.*, 2016, **3**, 425-440. [[Link](#)]
- 20 Feng Q.L.; Wu J.; Chen G.Q.; Cui F.Z.; Kim T.N.; Kim J.O. A Mechanistic Study of the Antibacterial Effect of Silver Ions on *Escherichia coli* and *Staphylococcus aureus*. *J. Biomed. Mater. Res.*, 2000, **52**, 662-668. [[CrossRef](#)]
- 21 Berger T.J.; Spadaro J.A.; Bierman R.; Chapin S.E.; Becker R.O. Antifungal Properties of Electrically Generated Metallic Ions. *Antimicrob. Agents Chemother.*, 1976, **10**, 856-860. [[CrossRef](#)]
- 22 Stoimenov P.K.; Klinger R.L.; Marchin G.L.; Klabunde K.J. Metal Oxide Nanoparticles as Bactericidal Agents. *Langmuir*, 2002, **18**, 6679-6686. [[CrossRef](#)]
- 23 Hamouda T.; Baker Jr J.R. Antimicrobial mechanism of Action of Surfactant Lipid Preparations in Enteric Gram-Negative Bacilli. *J. Appl. Microbiol.*, 2000, **89**, 397-403. [[CrossRef](#)]
- 24 Sondi I.; Goia D.V.; Matijević E. Preparation of Highly Concentrated Stable Dispersions of Uniform Silver Nanoparticles. *J. Colloid Interf. Sci.*, 2003, **260**, 75-81. [[CrossRef](#)]



© 2021, by the authors. Licensee Ariviyal Publishing, India. This article is an open access article distributed under the terms and conditions of the Creative Commons Attribution (CC BY) license (<http://creativecommons.org/licenses/by/4.0/>).